Highly Fluorescent *N*,*N*-Dimethylaminophenylethynylarenes: Synthesis, Photophysical Properties, and Electrochemiluminescence

Tong-Ing Ho,* Arumugasamy Elangovan, Hsien-Yi Hsu, and Shu-Wen Yang

Department of Chemistry, National Taiwan University, Taipei - 106, Taiwan

Received: December 7, 2004; In Final Form: February 25, 2005

A new family of aryl-π-donor-aryl molecules has been synthesized and studied with respect to their photophysical properties and electrogenerated chemiluminscence (ECL) for the first time. Anthracene, phenanthrene, naphthalene, biphenyl, and fluorene were coupled with *N*,*N*-dimethylanilino moiety via a C−C triple bond (**1**−**7**). Introduction of such a strong electron-donating moiety as *N*,*N*-dimethylanilino group through a triple bond imparts new properties to the resultant molecules that are not commonly observed for the parent arenes. All molecules show absorption in the near-visible region and emission totally in the visible region with high fluorescence quantum yields. Bright solid-state photoluminescence has also been noticed for all the compounds in the visible region. 9-Anthryl- and 1-naphthyl- derivatives exhibited blue-shifted electrochemiluminescence (ECL) relative to their photoluminescence because of aggregation. 9-Phenanthryl- and 2-naphthyl-derivatives did not show ECL. 2-Biphenyl derivative showed monomeric ECL while 4-biphenyl counterpart exhibited excimer ECL. No ECL was observed for 2-fluorenyl derivative. The observed electronic properties are discussed with regard to the structure of the molecules. The characteristics of the molecules chosen in the present study open up new prospects and promises for novel tunable organic materials, on the basis of simple extension of conjugation to promote intramolecular communication, for ECL, OLED, and other optoelectronic applications.

Introduction

Architecture of π-conjugated aromatic compounds assumes significance in view of the application of these compounds in nonlinear optics (NLO),[1] in organic light-emitting diodes (OLEDs),[2] in polymer LEDs, in carbohydrate sensors,[3] in electrogenerated chemiluminescence (ECL),[4] as photoconductors,[5] and in molecular electronics and other optoelectronic applications.[6] Design and synthesis of diarylethyne compounds by catalytic cross-coupling of terminal acetylenes with aryl halides are the latest strategies in this endeavor. Coupling of donor-arylethynyl moieties with common acceptor aromatic fluorophores would enable us to achieve new molecules with bipolar centers. Such compounds are called organic mixed-valence compounds[7] and are useful probes for adiabatic electron-transfer processes, and their novel properties would make them suitable candidates for the said application. Polycyclic aromatic compounds such as fluorene, biphenyl, naphthalene, anthracene, and phenanthrene are well-known emitters and their photophysical properties have been well-established and well-exploited for various applications. Several reports have appeared on the extensive photophysical studies of donor−acceptor biaryl compounds linked by a C−C single bond with respect to their intramolecular electron-transfer interactions.[8] While complex macromolecules and electron-rich dendrimers based on ethyne have been well-studied, it is rather surprising that little is known of such simple systems as unsymmetrical diarylethynes (Scheme 1), and yet they appear to be useful for the said studies and applications.

Annihilation of radical ions which are generated sequentially, with a time interval, at the vicinity of electrodes, can lead to emission of light of certain wavelength. This phenomenon is called electrogenerated chemiluminescence (ECL).[9] ECL can be observed either from a singlet or from a triplet state of the electroactive species and can be formed depending on the annihilation enthalpy change ($\Delta H°$) during the electron-transfer reaction. The ion annihilation can generate singlet state (S-route)[9a,g] if the magnitude of $\Delta H°$ is sufficiently larger than the energy needed for the excited singlet state (S_1). On the other hand, if the $\Delta H°$ is lower than S_1, but it is sufficient to generate the triplet state, then the electron-transfer reaction will lead to the formation of triplet state. However, it is yet possible to achieve singlet state by triplet−triplet annihilation, and this is known as a T-route.[9g] As a result, the light emitted from the electrochemically generated excited state of electroactive species normally is fluorescence.

We have studied the ECL of a series of intramolecular charge transfer (ICT) donor−acceptor stilbenoid systems bearing *N*,*N*-dialkylamino group as donor and pyridyl, thiophenyl, and aryl as acceptors. Most of the stilbenoids showed ICT−ECL through direct annihilation of radical ions. Only for poor ICT compounds with weaker electron demanding thiophene, excimer ECL was observed.[4a] ECL of donor-substituted phenylquinolinylethynes have been studied by us, and we have found out that the coplanarity of the donor and quinolinyl acceptor moieties along the triple bond plays a role in determining the type and emission wavelength of the ECL.[4b] Study of ECL in solution is fundamental to the electroluminescence (EL) in solid state as the process of generation of excited states in EL and ECL is the same.[9e,10] Hence, the present study of electrochemiluminescence of π-extended chromophores together with general optical properties in solution, especially the luminescence, assumes significance to the organic materials chemists. More-

* Author to whom correspondence should be addressed. Fax:+886-2-2363-6359; tel: +886-2-2369-1801; e-mail: hall@ntu.edu.tw.

10.1021/jp0444518 CCC: $30.25
Published on Web 04/02/2005

SCHEME 1: Synthesis of the Fluorophores 1−7 by Coupling of Bromoarenes with *p*-*N*,*N*-Dimethylanilinoalkyne

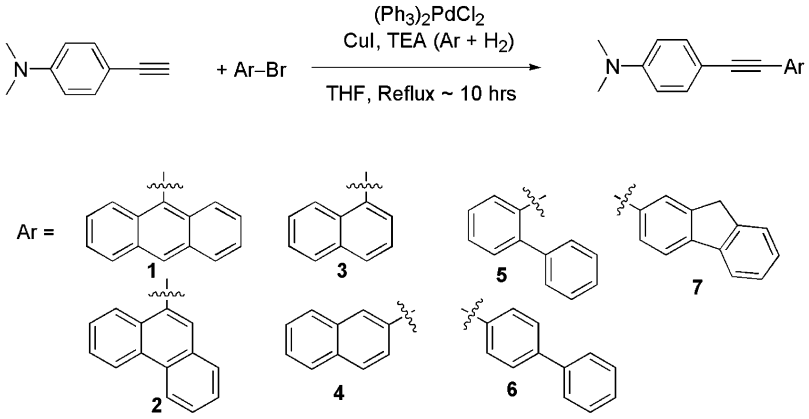

over, the possibility of generation of uncommon excited states by comproportionation of electrogenerated encounter complexes as observed by us[4c−4e] and others[10c] is substantiated in this work.

For the present objective, the molecules shown as products in Scheme 1 were chosen to study the ECL properties in addition to studying the ability to tuning the general photophysical properties. We have chosen the *N*,*N*-dimethylanilino group as a common electron donor moiety and have varied the polyaromatic fluorophore moieties (electron acceptors) to study the steric and electronic effects on the ECL and overall photophysical properties.

Experimental Section

Materials. All the chemicals and reagents were purchased from Acros Organics and were used as received unless specified otherwise. Dicholobis(triphenylphosphine)palladium(II) was either prepared in-house or from commercial source (Acros). Solvents were distilled as per the standard methods and purged with argon before use. Triethylamine (TEA) and tetrahydrofuran (THF) were distilled and purged with a mixture of approximately 1:1 argon and hydrogen before use.

Methods. Characterization. Proton NMR spectra of the samples were recorded with 400 MHz Varian instrument and ^{13}C NMR spectra were recorded with the same instrument at 100.1 MHz operator frequency in $CDCl_3$ solvent (Merck) with $CHCl_3$ internal standard (δ 7.24 ppm for ^{1}H and 77 ppm, middle of the three peaks, for ^{13}C spectra). Mass spectra were recorded with JEOL SX 102A instrument on nitrobenzyl alcohol matrix. TLC was run on Merck precoated aluminum plates (Si 60 F_{254}). Column chromatography was run on Merck silica gel (60−120 mesh) and neutral alumina (Merck) 70−230 mesh.

Photophysical Measurements. All UV−vis spectra were recorded on HITACHI U-2000 spectrophotometer with 10 μM solution of the compounds in CH_3CN and all fluorescence spectra on HITACHI F-3010 fluorescence spectrophotometer using similar solution concentrations. Quantum yields were determined using coumarin 334 as standard (Φ = 0.69 in MeOH).[11] The quantum yields were calculated using the equation[12]

$$\Phi_x = \Phi_s (A_s/A_x) (I_x/I_s) (n_x/n_s)^2 \qquad (1)$$

where Φ_x is the quantum yield of unknown, Φ_s is that of standard, A_s is the absorbance of standard, A_x is that of unknown, I_s is the integrated area of fluorescence intensity of standard, I_x is that of unknown, and n_x and n_s are the refractive indices of solvent used for the unknown and standard, respectively. The concentrations of the unknown samples were adjusted such that the absorbance becomes equal to that of the standard (A = 0.2). Further, the point of intersection of the maxima of standard and the unknown was chosen as excitation wavelength. In consequence, the absorbance terms required for the calculation (i.e., A_r/A_s) in the equation attains unity. However, the absorbance values were incorporated in the calculation of Φ in the solvatochromic studies. Solvatochromic studies were done on Cintra10c UV−Vis Spectrophotometer and Aminco-Bauman Luminescence spectrometer. Solid-state fluorescence spectra were recorded with thin solid films of the compound cast from methylene chloride solutions on a 1 cm × 1 cm quartz plate. The excitation wavelength for **1** was 430 nm and that for the rest was 320 nm.

Electrochemical and ECL Measurements. CV measurements were done on CH Instruments Electrochemical Analyzer for solutions of the compound in deaerated acetonitrile with a scan rate of 50 mV/s. The cell used was a three-electrode cell consisting of a carbon disk (2.0 mm) working electrode, a platinum wire counter electrode, and a Ag/AgCl reference electrode. ECL spectra were recorded at room temperatures using a setup consisting of F-3010 Fluorescence spectrophotometer, CV-27 Voltammograph using Pt wire (0.25-mm diameter, Aldrich) and Pt gauss (100 mesh (Aldrich), 0.5 cm × 0.5 cm) electrodes together with a Ag/AgCl reference electrode with a computer interface to control the pulsing. The electrode surfaces were prepared freshly before CV and ECL experiments. Carbon disk electrode was rubbed against alumina paste followed by rinsing with double-distilled water and MeCN and wiping with high-quality lint-free tissue (Kimberly-Clark delicate wipers). The Pt wire and the Pt gauss electrodes were cleaned by rinsing with dilute nitric acid followed by water, and then they were finally fired with a naked flame to ensure maximum cleanliness of the electrode. A 1 mM concentration of the compound in dry degassed acetonitrile along with 0.05 M tetrabutylammonium perchlorate (TBAP) and the solution was degassed by purging it with dry argon for both CV and ECL measurements. To generate annihilation reaction for ECL, the platinum electrodes were pulsed between first reduction and first oxidation potentials, and the pulse interval was controlled on a computer. All measurements were done at room temperatures (22−23 °C).

General Synthetic Procedure. Compounds **1**−**7** were prepared by modified Sonogashira coupling reaction[13] of *N*,*N*-dimethylaminophenylethyne with the respective bromoarenes. Synthesis of **1** is typical: To a two-neck round-bottomed flask equipped with a reflux condenser was placed a stirring bar, 9-bromoanthracene (257 mg, 1 m mol), CuI (4 mg, ~2 mol %), and dichlorobis(triphenylphosphine)palladium(II) catalyst

(14 mg, 2 mol % relative to the bromoarene used), and the whole setup was degassed and back-filled three times with a gaseous mixture of 1:1 hydrogen and argon. THF (8 mL) was introduced via a syringe followed by TEA (6 mmol). The reaction mixture was set to heat to about 60 °C and then a solution of the *N*,*N*-dimethylaminophenylethyne (145 mg) in 5 mL THF was introduced under the reducing atmosphere. The reaction was followed by TLC and, when complete (about 10 h), the solvents were evaporated and the residue was chromatographed on silica gel column to get pure 9-(4-*N*,*N*-dimethylaminophenyl)ethynyl-anthracene **1** (292 mg) in 89% yield.

Characterization Data. 9-(4-*N*,*N*-Dimethylaminophenyl)-ethynylanthracene (1). mp: 180−183°C; ^{1}H NMR (400 MHz; δ ppm, $CDCl_3$; with $CHCl_3$ internal standard δ 7.24 ppm) 8.66 (d, J = 8.8 Hz, 2H), 8.35 (s, 1H), 7.98 (d, J = 8.8 Hz, 2H), 7.64 (d, J = 8.4 Hz, 2H), 7.57 (t, J = 7.6 Hz, 2H), 7.50 (t, J = 7.6 Hz, 2H), 6.74 (d, J = 8.8 Hz, 2H), 3.03 (s, 6H); ^{13}C NMR (100 MHz, $CDCl_3$; δ ppm): 150.12, 132.66, 132.11, 131.15, 128.44, 126.93, 126.43, 126.04, 125.45, 118.36, 111.86, 110.35, 102.25, 84.34, 40.35. H. R. mass (M^+): 321.1512 (calculated M^+: 321.1517). The data for the rest of the compounds are given below.

9-(4-*N*,*N*-Dimethylaminophenyl)ethynylphenanthrene (2). Yield 73%; mp: 170−173 °C; ^{1}H NMR ($CDCl_3$) δ ppm: 8.71−8.60 (m, 3H), 8.07 (s, 1H), 7.87 (d, J = 7.6 Hz, 1H), 7.74 (d, J = 6.2 Hz, 2H), 7.72−7.59 (m, 2H), 7.58 (d, J = 8.8 Hz, 2H), 6.71 (d, J 8.8 Hz, 2H), 3.02 (s, 6H);^{13}C NMR ($CDCl_3$) δ ppm: 150.01, 132.68, 131.34, 131.14, 130.62, 129.96, 129.79, 128.22, 126.99, 126.84, 126.75, 126.69, 122.56, 122.43, 120.40, 111.77, 109.95, 95.37, 85.67, 40.24. HRMS (M^+): 321.1513 (calculated M^+: 321.1517).

1-(4-*N*,*N*-Dimethylaminophenyl)ethynylnaphthylene (3). Yield 70%; mp: 89−91 °C; ^{1}H NMR ($CDCl_3$) δ ppm: 8.46 (d, J = 8.4, 1H), 7.84 (d, J = 7.2 Hz, 1H), 7.82 (d, J = 7.5 Hz, 1H), 7.75 (d, J = 8.2 Hz, 1H), 7.58 (t, J = 6.8 Hz, 1H), 7.56 (d, J = 8.5 Hz, 3H), 7.42 (t, J = 6.99 Hz, 1H), 6.68 (d, J = 8.3 Hz, 2H), 2.98 (s, 6H); ^{13}C NMR ($CDCl_3$) δ ppm: 150.33, 133.42 133.39, 132.95, 129.82, 128.37, 128.03, 126.65, 126.63, 126.43, 125.50, 122.30, 112.11, 110.42, 95.96, 85.78, 40.62; HRMS (M^+): 271.1355 (calculated M^+: 271.1361).

2-(4-*N*,*N*-Dimethylaminophenyl)ethynylnaphthylene (4). Yield 88%; mp: 93−96 °C; ^{1}H NMR ($CDCl_3$) δ ppm: 8.00 (s, 1H), 7.79−7.75 (m, 3H), 7.56 (d, J = 8.8 Hz, 1H), 7.43 (d, J = 8.3 Hz, 4H), 6.67 (d, J = 8.2 Hz, 2H), 2.97 (s, 6H); ^{13}C NMR ($CDCl_3$) δ ppm: 149.95, 133.01, 132.63,, 132.30, 130.50, 128.37, 127.68, 127.57, 127.51, 126.23, 126.07, 121.39, 111.76, 109.93, 91.05, 87.77, 40.27; HRMS (M^+): 271.1356 (calculated M^+: 271.1361).

2-(4-*N*,*N*-Dimethylaminophenyl)ethynyldiphenyl (5). Yield 65%; mp: 105−109 °C; ^{1}H NMR ($CDCl_3$) δ ppm: 7.72 (d, J = 7.2 Hz, 2H), 7.62 (d, J = 7.8 Hz, 1H), 7.48−7.31 (m, 6H), 7.20 (d, J = 8.2 Hz, 2H), 6.62 (d, J = 8.0 Hz, 2H), 2.97 (s, 6H); ^{13}C NMR ($CDCl_3$) δ ppm: 149.69, 142.94, 140.55, 132.23, 132.14, 129.24, 129.16, 127.59, 127.46, 127.07, 126.78, 122.23, 111.58, 110.06, 93.51, 87.29, 40.15; HRMS (M^+): 297.1500 (calculated M^+: 297.1517).

4-(4-*N*,*N*-Dimethylaminophenyl)ethynyldiphenyl (6). Yield 92%; mp: 97−99 °C; ^{1}H NMR ($CDCl_3$) δ ppm: 7.58 (d, J = 7.6 Hz, 2H), 7.54 (m, 4H), 7.45−7.40 (m, 4H), 7.34 (t, J = 7.2 Hz, 1H), 6.66 (d, J = 8.8 Hz, 2H), 2.98 (s, 6H); ^{13}C NMR ($CDCl_3$) δ ppm: 149.93, 140.36, 139.92, 132.59, 131.52, 128.62, 127.29, 126.83, 126.77, 122.99, 111.76, 109.98, 91.31, 87.24, 40.31; HRMS (M^+): 297.1513 (calculated M^+: 297.1517).

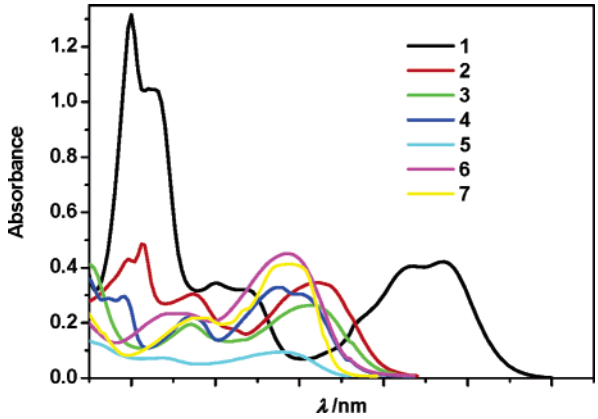

Figure 1. UV−vis spectra of **1**−**7** in CH_3CN (1.0×10^{-5} M).

2-(4-*N*,*N*-Dimethylaminophenyl)ethynylfluorene (7). Yield 79%; mp: 171−175 °C; ^{1}H NMR ($CDCl_3$) δ ppm: 7.75 (d, J = 7.2 Hz, 1H), 7.72 (d, J = 8.0 Hz, 1H), 7.67 (s, 1H), 7.54−7.51 (m, 2H), 7.43 (d, J = 8.6 Hz, 2H), 7.39 (t, J = 7.8 Hz, 1H), 7.30 (t, J = 7.2 Hz, 1H), 6.66 (d, J = 8.8 Hz, 2H), 3.89 (s, 2H), 2.98 (s, 6H); ^{13}C NMR ($CDCl_3$) δ ppm: 149.82, 143.31, 142.95, 141.09, 140.91, 132.52, 129.98,127.66, 126.74, 126.70, 124.89, 122.09, 119.90, 119.58, 111.70, 110.13, 90.58, 88.04, 40.29, 36.81; HRMS (M^+): 309.1505 (calculated M^+: 309.1517).

Theoretical Calculations. Spartan'04 was used as a platform to calculate HOMO and LUMO levels with density functional theory (DFT) using Beck's three-parameter Lee−Yang−Parr (B3LYP) level of theory with 6-31G* basis set of functions as provided by Spartan'04 for Windows, Wave function Inc., Irvine, CA 92612. Molecules were optimized in the gas phase at ground state throughout.

Results and Discussion

Compounds **1**−**7** were obtained by the catalytic cross-coupling of *N*,*N*-dimethylaminophenylethyne with corresponding aryl bromides in satisfactory to high yields using modified Sonogashira reaction.[13] The yields of **1**−**3** have been substantially increased when conducting the reaction under dilute hydrogen atmosphere despite the steric interaction caused by the *peri*-hydrogens on these rings and that of **5** was relatively low because of steric demand while **4**, **6**, and **7** were prepared in very good yields. All the compounds were characterized by ^{1}H NMR, ^{13}C NMR, and HR−FAB mass spectra.

Photophysical Studies. The UV−vis and solution photoluminescence spectra of **1**−**7** (1.0×10^{-5} M) were recorded in CH_3CN solution and the UV−vis spectra are shown in Figure 1 (see also Table 1 for values). The $\pi-\pi^*$ transitions for **2**−**7** appear close to the visible region while the β-band absorptions appear near 230 nm. The longest wavelength absorption maximum of **1** which appears as a structured anthracene-like band has been pushed into the visible region. The rest of the compounds in the series show almost structureless charge-transfer band close to the visible region with the onset of absorption at about 400 nm. Compound **5** shows the weakest absorption probably because of high-symmetry demand.

Compounds **6** and **7** absorb strongly (cf. ϵ_{max}, Table 1) and they emit strong blue-violet fluorescence in ACN with high quantum yields (Φ^{flu}, Table 1 and Figure 2. Both the absorption and emission maxima of **1** have the longest wavelength among all. Although compounds **1**−**4** and **6** apparently exhibit Stokes shift 22 nm higher than those of **5** and **7**, actually the energy units ($\Delta\nu$ in cm^{-1}) reveal that the compounds **2**−**5** exhibit higher

TABLE 1: Photophysical Data of 1−7 in CH_3CN Solution and Solid-State Fluorescence

compound	λ_{max}^{abs}/nm [ν/cm^{-1}]	ϵ_{max}[a]	λ_{max}^{Flu}/nm [ν/cm^{-1}]	Stokes shift $\Delta\nu$/cm^{-1}	Φ^{flu}[b]	λ_{max}^{ECL}/nm	$\lambda_{max}^{Flu(S)}$[c]/nm
1	436 [22 936]	4.22	563 [17 762]	5174	0.18q	537	525
2	358 [27 933]	3.45	488 [20 492]	7441	0.26		525
3	356 [28 090]	2.46	484 [20 661]	7428	0.24	441	458
4	350 [28 571]	3.05	472 [21 186]	7385	0.35		461
5	340 [29 412]	0.95	447 [22 371]	7040	0.25	457	410
6	344 [29 070]	4.51	472 [21 186]	7883	0.43	517	430
7	349 [28 653]	4.12	452 [22 124]	6529	0.59		423

[a] ($\times 10^4$ M^{-1} cm^{-1}). [b] Quantum yields (Φ^{flu}) were determined in CH_3CN using coumarin 334 as standard ($\Phi = 0.69$ in MeOH).[11] [c] Solid-state fluorescence.

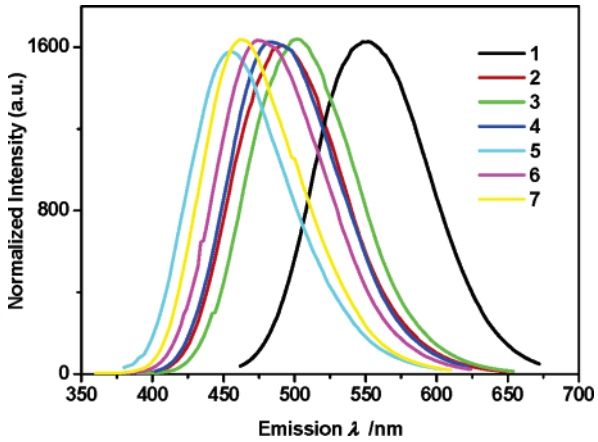

Figure 2. Fluorescence spectra of **1**−**7** in CH_3CN (1.0×10^{-5} M).

energy difference than **1** and **6**. Larger Stokes shift generally implies more prominent charge transfer in the excited state of the former than in that of the latter which indicates better stabilization of the excited state for **2**−**5**. All compounds have very high fluorescence quantum yields and the Φ^{flu} of **7** is the highest in the series. Fluorescence spectra of all the compounds show emission maxima in the visible region in ACN solution. While none of the unsubstituted free arenes in this series show visible light emission, it is interesting and useful that the efficient charge transport supported by strong electronic coupling between the donor and acceptor through C−C triple bond brings down the HOMO−LUMO energy gap and emits visible light.

Among **1**−**7**, **1** and **2** exhibit solvatochromism in the visible region (with **1** being more intensely colored than **2**), blue in hexane, blue-green in benzene, green in THF, greenish-yellow in methylene chloride, yellow in ethanol, yellow in acetonitrile, and orange in DMSO under visible light and with higher fluorescence intensity under black light (see the Supporting Information for color pictures). The absorption maxima recorded in various solvents reveal moderate shift to the red from 435 nm in hexane to 445 nm in DMSO for **1** upon increasing the polarity of the solvent (see Table 2). There is a well-pronounced increase in the Stokes shift and decrease in emission quantum yield with increase in polarity of the solvent. The display of emission colors is depicted in Figure 3 in the form of spectra recorded for compound **1** in various solvents. As can be seen from the spectra, the emission maxima shift from initial structured band in hexane at 448 nm to a structureless band at lower energy upon increasing the solvent polarity from hexane to DMSO (586 nm).

A chromophore in an environment is described as a dipole in a sphere of radius *a*, with a dipole moment μ at ground state and μ^* in the excited state. The interaction between the chromophore and the solvent affects the energy difference between the ground and excited states. This energy difference,

TABLE 2: Solvatochromic Data of 1

solvent (ϵ)[a]	λ_{max}^{abs}/nm [ν/cm^{-1}]	ϵ_{max}[b]	λ_{max}^{Flu}/nm [ν/cm^{-1}]	Stokes shift/ $\Delta\nu$ cm^{-1}	Φ^{Flu}[c]
hexane (1.89)	435 [22 988]	1.38	448 [22 321]	667	0.80
benzene (2.28)	445 [22 472]	2.62	481 [20 790]	1682	0.78
THF (7.52)	439 [22 779]	2.80	521 [19 193]	3585	0.54
CH_2Cl_2 (9.08)	440 [22 727]	2.70	521 [19 194]	3533	0.54
ethanol (24.30)	432 [23 148]	1.40	536 [18 657]	4491	0.25
ACN (37.5)	435 [22 988]	2.14	562 [17 794]	5195	0.18
DMSO (48.9)	445 [22 471]	3.05	586 [17 065]	5407	0.11

[a] Dielectric constant (ϵ, from ref 23). [b] ($\times 10^4$ M^{-1} cm^{-1}). [c] Φ^{Flu} calculated using coumarin 334 as standard.[11]

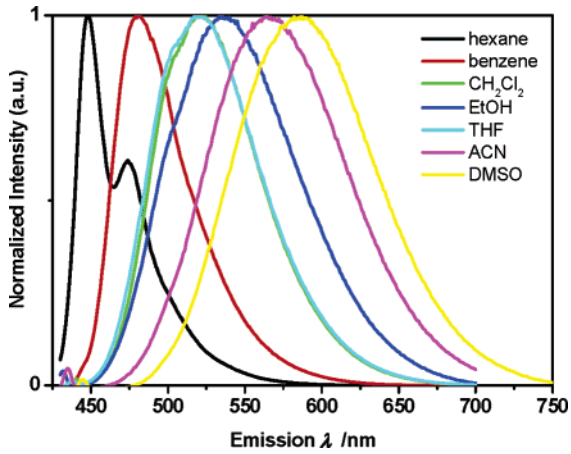

Figure 3. Normalized photoluminescence spectra of **1** in various solvents.

implied by the Stokes shift (in cm^{-1}), is a property of the refractive index (n) and the dielectric constant (ϵ) of the solvent used. The influence of local molecular environment on the optical property of **1**, for example, can be understood by using the Lippert equation, a model that describes the interactions between the solvent and the dipole moment of chromophore.[14]

$$\nu_{abs} - \nu_{Flu} = 2/hc[\Delta f]\{(\mu^* - \mu)^2/a^3\} + \text{constant} \quad (2)$$

where

$$\Delta f = [(\epsilon - 1)/(2\epsilon + 1)] - [(n^2 - 1)/(2n^2 + 1)] \quad (3)$$

A plot of polarity (or the orientation polarizability, Δf) of the solvents against the Stokes shift for compound **1** in various solvents is shown in Figure 4. The observed linear correlation between the Stokes shift and the Δf illustrates the adherence of experimental data to the Lippert equation. The excited states for the rest of the compounds can be assumed to be better stabilized than **1** as well as their unsubstituted counterparts owing to the observed larger Stokes shift (>5000 cm^{-1}).

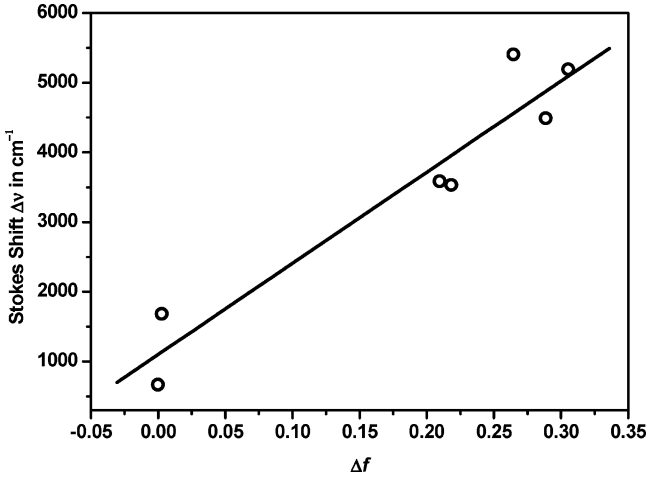

Figure 4. Linear plot of Stokes shift verses orientation polarizability (Δf) of the medium for **1** in various solvents.

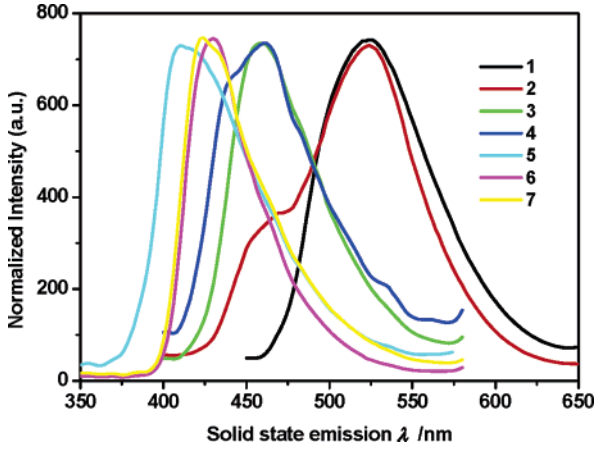

Figure 5. Normalized solid-state fluorescence spectra of **1**−**7** recorded from solution cast thin crystalline solid film on quartz slides.

TABLE 3: Electrochemical Data of 1−7 in CH_3CN Solution

compound	$E_{p,RED}$/V	$E_{p,OX}$/V	$-\Delta H°$/eV	λ_{max}^{ECL}/eV
1	−0.93	0.83	1.60	2.30
2	−0.93	0.82	1.59	
3	−0.88	0.85	1.57	2.81
4	−0.90	0.83	1.57	
5	−0.89	0.88	1.61	2.71
6	−0.88	0.84	1.56	2.39
7	−0.87	0.82	1.53	

We observed bright emission of light upon shining black light on solid samples of **1**−**7**, and hence recording a qualitative emission spectra would be worthwhile. Figure 4 shows the emission spectra of **1**−**7** recorded from thin crystalline films. When compared with solid-state emission spectra, the solution photoluminescence spectral maxima were shifted to the red by about 10−40 nm. This indicates that there is a little interaction between the solvent and solute in high polar acetonitrile as is natural and consistent with the environment dependency of the emission. In Figure 5, a shoulder at 470 nm is noticed for **2** which can appear because of emission from the monomer while the maximum at 525 nm can be ascribed to the excimer emission. Although the thickness of the solid films were not optimized and the nature of the film may be amorphous in some cases, we are currently satisfied with the qualitative observation of solid-state emission spectra exhibiting somewhat close consistency with the solution fluorescence spectra.

Electrochemical and ECL studies. Cyclic voltammetry was employed to study the electroactivity and to determine the redox

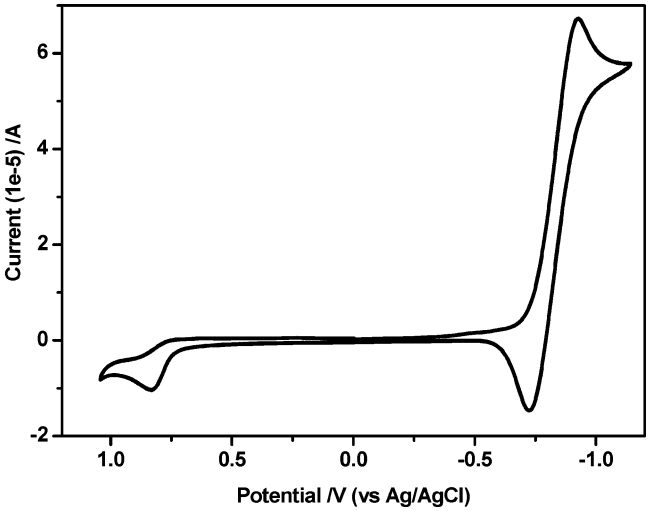

Figure 6. Cyclic voltammogram of **1** in CH_3CN (1.0×10^{-3} M with 50 mM TBAP) at a scan rate of 50 mV/s.

potential values of these mixed valence systems. All compounds exhibit very much reversible reduction curves and quasi-reversible/irreversible oxidation curves. The first reduction and oxidation potentials which correspond to the reduction of the arenes and *N*,*N*-dimethylaminophenyl moieties, respectively, are recorded in Table 3. There is very little variation in the oxidation potential values among **1**−**7**, as the donor is the same, but there is a moderate variation in the reduction potential values. This reflects the change in the LUMO energy level upon varying the acceptor arene. Comparing the observed reduction potential values in Table 3 with the reported half-wave reduction potential values of free arenes (anthracene, −1.94; phenanthrene, −2.45; naphthalene, −2.5; biphenyl, −2.7; and fluorene, −2.64 in volts),[15] it can be seen that there is a drastic lowering of the values suggesting strong electronic coupling between the donor and acceptor groups. The enthalpy change for the radical ion annihilation reaction ($-\Delta H°$) was calculated from the oxidation and reduction potentials using the equation[16]

$$-\Delta H^0 = E_{P,OX} - E_{P,RED} - 0.16\ \text{eV} \qquad (4)$$

and are recorded in Table 3 and a typical CV curve for **1** is shown in Figure 6.

The ECL spectra were recorded between −0.8 V (2s) and +0.93 V (2 s) with 0.9-s intermission and the ECL maxima for **1**−**7** are summarized in Table 1. Compounds **1**, **3**, **5**, and **6** exhibit ECL character while **2**, **4**, and **7** failed. Change of applied potentials by 100 mV negative to the peak or applying half-wave potential showed similar response suggesting that the ECL active compounds showed ECL with minor change in the shape without shift in the maxima while ECL inactive compounds remain indeed inactive under changed conditions. The ECL emission maxima of compounds **1** and **3** are blue-shifted when compared with solution photoluminescence maxima. The annihilation products emit higher energy than the photoexcited species. This follows the similar trend as observed earlier for *p*-donor-substituted phenylethynyl-4-quinolines,[4c] phenylethynyl-acridines,[4d] and phenylethynylcoumarins[4e] and in certain other oppositely π-stacking donor−acceptor systems. In addition, there are a few reports of reduction in the emission intensity with blue shift in the maxima of excimer fluorescence of 9-anthronitrile.[17] Hence, the state of the ECL emitting species may be proposed to have a special kind of structure, a bimolecular aggregate in which the polynuclear arene moieties are stacked

SCHEME 2: Proposed Structure of the Aggregate for 1

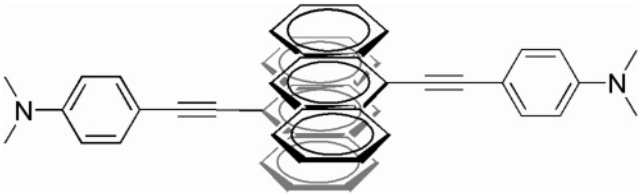

SCHEME 3: Probable Mechanism for the Formation of Aggregate for 1 and 3

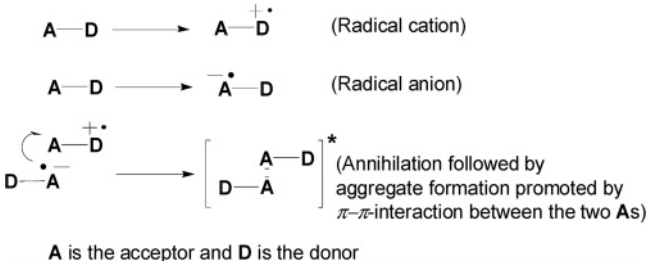

face-to-face with *N*,*N*-dimethylaminophenyl groups projecting perpendicularly away from each other in the opposite direction (as in Scheme 2). This type of aggregate formation during annihilation reaction may be responsible for the ECL emission blue-shifted with respect to the photoluminescence, and the mechanism for its formation may be as shown in Scheme 3.

Although the extension of π-conjugation does induce red shift (and larger Stokes shift) in the photoluminescence spectra compared to free anthracene, the ECL of **1** does not show red-shifted ECL to the same extent as with photoluminescence spectra. Unsubstituted anthracene shows ECL at 450 nm in ACN, and this has been assigned to excimer[18a,b] though, in DMF, the cation radical underwent reaction to form anthranol whose ECL was observed at 457 nm.[18c] In **1**, we observed only a blue shift rather than a red shift as compared to its photoluminescence maximum. Had there been any such reaction product formed under the ECL conditions, naturally we would have observed a red shift in its maximum. If a photodimer is formed alternatively, as is common with anthracene, conjugation would be broken and there would be no ECL. Since the aggregate formation as depicted in Scheme 2 allows for $\pi-\pi$ interaction between the two anthracene units, efficient packing may result in canceling out of dipole moment of the whole bimolecular assembly. Therefore, there may not be any net change except an increase in electron density at the center because of the presence of strong donors at remote. We can compare the reported excimer emission of anthracene in solution (540 nm)[19] with the aggregate emission (537 nm) observed in this study.

The fact that the ECL of **1** could well be repeated many times with the same sample solution in the ECL cell to observe neither shift in the position of the maximum nor reduction in intensity confirms that the ECL is from a fairly stable species and not from any decomposition or reaction side products. Further, when 1 mM concentration of the compound **1** was excited at 436 nm, the fluorescence was observed with much reduced (1/12) intensity and with slight broadening and without shift in the position of the emission maximum. Failure to observe blue shift in photoluminescence with high-concentration solution is probably because there is no annihilation between the neighboring molecules as in ECL conditions where annihilation between radical anion of one molecule and radical cation of a neighboring molecule takes place (Scheme 3). These observations suggest that the ECL emissive state has a unique structure that is quite different from the photoluminescent state. These details support

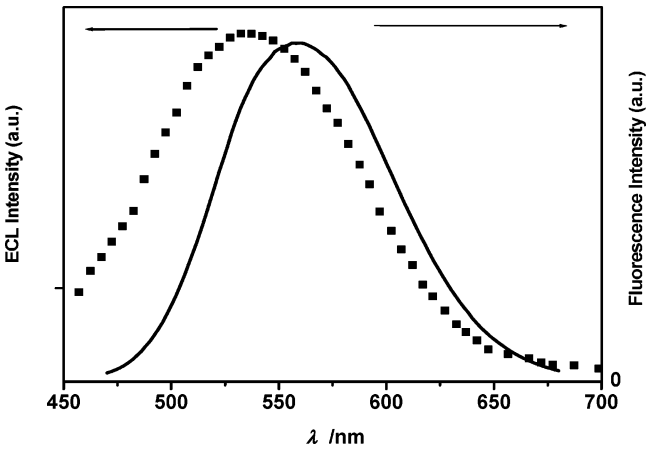

Figure 7. ECL (squares) spectrum of **1** showing blue shift with respect to its photoluminescence spectrum (solid line).

our notion of formation of aggregate for **1** in solution during annihilation reaction under the ECL experimental conditions. A typical graph of comparative ECL and fluorescence spectra of **1** is shown in Figure 7.

X-ray crystal structure analysis was carried out for compound **1** to get an insight into the packing in the ground state.[20] Figure 8 shows the packing arrangement from which one can see the donor-bearing phenyl group projecting in a near-perpendicular fashion relative to the anthracene moiety. The dihedral angle between the plane of the donor-bearing phenyl group and that of the anthracene group was determined to be 73.7°, and the interplanar distance between the two offset-parallel anthracene planes of adjacent molecules was measured to be 3.48 Å which is typical of $\pi-\pi$ interaction. This arrangement supplements our concept of the tendency of this kind of molecules undergoing aggregate formation under suitable conditions at sufficiently higher concentrations used for ECL measurements and under annihilation condition.

Compound **3** shows ECL maxima at 441 nm which is about 40 nm higher than the known excimer photoluminescence reported for free naphthalene[21] but 47 nm lower than its own photoluminescence maximum. This difference may be due to the inefficient packing in the formation of the bimolecular complex of the ECL emitting species leading to poor $\pi-\pi$ interaction.

Compound **5** exhibits monomer ECL presumably due to twisted ICT behavior because of its twisted nature while **6** exhibits excimer ECL as is evident from the larger red shift compared to the photoluminescence maximum. Various effects such as steric and electronic (resonance) effects can play a role in determining the ECL activity. The radical ions, especially the radical anion, of compounds **2**, **4**, and **7** may not be stable enough to undergo annihilation reaction to produce an excited state. In fact, small discoloration of the solution was noticed in the cell during ECL study. In **2** and **4**, the radical anion can be construed as formed and localized on the acceptor rings and reacts with the environment to get decomposed without emitting photons. In **7**, even though the fluorenyl moiety is rigid and planar, the bent caused by the rigidification due to methylene bridge likely prevents ICT, and hence no ECL was observed.

To understand the mechanism of excited-state formation (S-route/T-route) of ECL emission, the enthalpy change of annihilation reaction ($-\Delta H°$) can be compared with the energy of ECL emission. From Table 3 it can be found that the energy provided by the annihilation of radical anions and radical cations is not sufficient to populate the singlet states for these

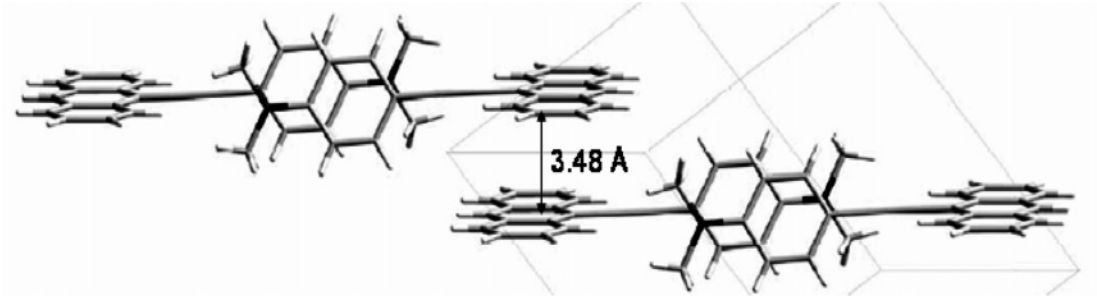

Figure 8. Crystal packing diagram of **1** showing $\pi-\pi$ interaction between the two adjacent anthracene moieties with an interplanar distance of 3.48 Å.

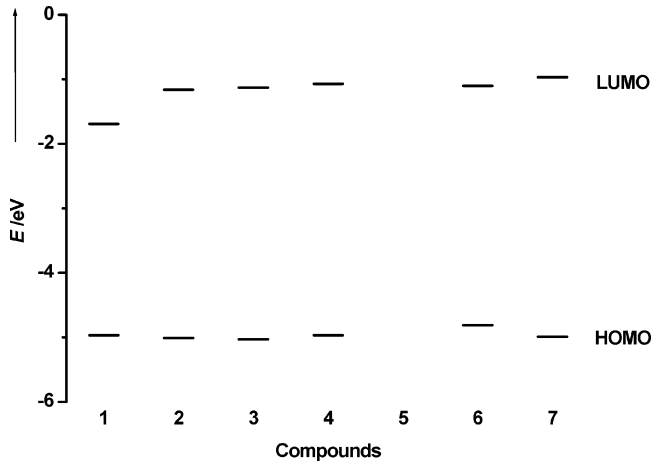

Figure 9. Calculated HOMO−LUMO energy levels for compounds **1**−**4**, **6**, and **7**. Calculations were done at B3LYP/6-31G* level using Spartan '04 program.[22] Attempted optimization of **5** failed under similar conditions of calculations.

compounds (**1**−**7**). Thus, the ECL emission energy must have been derived from the triplet states. A triplet−triplet annihilation process must have taken place (T-route) for the ECL active systems (**1**, **3**, **5**, and **6**). For ECL inactive systems (**2**, **4**, and **7**), low yields of the radical ions may have contributed to the ECL inactivity in addition to the structural arrangement disfavoring reaction of radical ions. Interestingly, no coreactant was employed in the present study, and therefore the observed ECL is from the direct annihilation process of radical ions. This is advantageous in that the common coreactants used in ECL studies in the cross-annihilation process[9f] are tertiary amines which quench emission.

To ascertain the observed electronic properties from the photophysical data and electrochemical data, we conducted theoretical calculations on all molecules using density functional theory (DFT).[22] Energies of HOMO and LUMO were calculated for molecules in the gas phase at ground state, and the calculated energy levels are compared in Figure 9. The HOMO−LUMO gap for **1** is the lowest among all as expected and the gap for all compounds except **5** agrees closely well with the experimental values obtained from the UV−vis spectra (Table 4). The slight difference between the calculated and experimental energy gap is plausible because the calculations were performed for molecules at gas phase while that UV−vis spectra were recorded in ACN solvent.

An extensive theoretical treatment requiring costly calculations would be necessary to provide a more comprehensive interpretation of the electronic structure of the ECL emissive species of **1** and related molecules which show blue-shifted ECL with respect to photoluminescence. Equally costly would be the treatment of molecules such as **5** which are highly unsymmetrical in nature.

TABLE 4: Calculated and Experimental HOMO−LUMO Energy for 1−4, 6, and 7

compound	E_{HOMO} (theory, eV)	E_{LUMO} (theory, eV)	$\Delta E_{HOMO-LUMO}$ (theory, eV)	$\Delta E_{HOMO-LUMO}$ (UV−vis, eV)
1	−4.97	−1.69	3.28	2.84
2	−5.01	−1.16	3.85	3.46
3	−5.03	−1.13	3.90	3.48
4	−4.97	−1.07	3.90	3.54
6	−4.81	−1.10	3.71	3.60
7	−4.99	−0.97	4.02	3.55

Conclusion

We have tailor-made new and simple ethyne-based highly fluorescence emitting molecules and studied their ECL and other photophysical properties. Emission properties can be altered at will by suitable substitution in the nucleus of fluorophores. While neither the arenes (except anthracene[9f]) nor the anilines are ECL active in their free forms, linking them with a π-bridge imparts ECL character to the resultant molecule, and no coreactant was required to generate ECL. Electron push into the rings imparted red shift in the photoabsorption and photoluminescence behavior of the π-extended arenes. High solution photoluminescence quantum yields and observation of solid-state fluorescence are salient features of the chosen mixed valence compounds.

Though the electrochemical characteristics do not show much variations among **1**−**7**, the ECL behavior is quite different. Compounds **1** and **3** show blue-shifted ECL emission compared to their photoluminescence. Compound **5** shows monomeric ICT ECL and **6** shows excimer ECL emission. Although there is no ECL activity for **2**, **4**, and **7**, the excellent fluorescence properties in solutions and in solid films of these and all the compounds in general would be useful for application as probes in analytical studies and in optoelectronic devices. The present study encourages further research into the origin of blue-shifted ECL as well as on design and application of unsymmetrical diarylethynes for the advancement of the fast expanding field of organic electronics in addition to establishing splendid structural groundwork. Use of these, and more new color-tunable organic materials in OLED, would be our future work.

Acknowledgment. Financial support by National Science Council, Taiwan, is gratefully acknowledged. We thank Prof. S. M. Peng, Mr. G. S. Lee, and Mr. Y. H. Liu for providing X-ray data for compound **1**.

Supporting Information Available: Proton and ^{13}C NMR spectra of all compounds and solvatochromic data and X-ray data for compound **1**. This material is available free of charge via the Internet at http://pubs.acs.org.

References and Notes

(1) For reviews on NLO materials, see: (a) *Nonlinear Optical Properties of Organic and Polymeric Materials*; Williams, D. J., Ed.; ACS Symposium Series 233; American Chemical Society: Washington, DC, 1983. (b) *Nonlinear Optical Properties of Organic Molecules and Crystals*; Chemla, D. S., Zyss, J., Eds.; Academic Press: New York, 1987; Vols. 1, 2. (c) *Organic Materials for Nonlinear Optics*; Hahn, R. A., Ed.; Spec. Publ. No. 69; The Royal Society of Chemistry: London, 1989. (d) *Organic Materials for Nonlinear Optics II*; Hahn R. A., Bloor, D., Eds.; Spec. Publ. No. 91; The Royal Society of Chemistry: Cambridge, U.K., 1991. (e) Prasad, P. N.; Williams, D. J. *Introduction to Nonlinear Optical Effects in Molecules and Polymers*; Wiley: Chichester, U.K., 1991. (f) Nalwa, H. S.; Miyata, S. *Nonlinear Optics of Organic Molecules and Polymers*; CRC Press: Boca Raton, FL, 1997. (*g*) Lesley, M. J. G.; Woodward, A.; Taylor, N. J.; Marder, T. B.; Cazenobe, I.; Ledoux, I.; Zyss, J.; Thornton A.; Bruce D. W.; Kakkar A. K. *Chem. Mater*, **1998**, *10*, 1355.

(2) For example, (a) Lee C.-H.; Yamamoto, T. *Tetrahedron Lett*. **2001**, *42*, 3993. (b) Matsumi, N.; Naka K.; Chujo, Y. *J. Am. Chem. Soc*. **1998**, *120*, 5112. (c) Wegner, G.; Müllen, K. *Electronic Materials-the Oligomer Approach*; Wiley-VCH: Weinheim, Germany, 1998. (d) Martin, R. E.; Diederich, F. *Angew. Chem., Int. Ed*. **1999**, *38*, 1350. (e) Odom, S. A.; Parkin, S. R.; Anthony, J. E. *Org. Lett*. **2003**, *5*, 4245.

(3) For example, (a) Fang, J.-M.; Selvi, S.; Liao, J.-H. Slanina, Z.; Chen, C.-T.; Chou, P.-T. *J. Am. Chem. Soc*. **2004**, *126*, 3559. (b) Inouye, M.; Takahashi K.; Nakazumi, H. *J. Am. Chem. Soc*. **1999**, *121*, 341.

(4) (a) Chen, C.-Y.; Ho, J.-H.; Wang, S.-L.; Ho, T.-I. *Photochem. Photobiol. Sci*. **2003**, *2*, 1232. (b) Elangovan, A.; Chen, T.-Y.; Chen, C.-Y.; Ho, T.-I. *Chem. Commun*. **2003**, 2146. (c) Elangovan, A.; Yang, S.-W.; Lin, J.-H.; Kao, K.-M.; Ho, T.-I. *Org. Biomol. Chem*. **2004**, *2*, 1597. (d) Elangovan, A.; Chiu, H.-H.; Yang, S.-W.; Ho, T.-I. *Org. Biomol. Chem*. **2004**, *2*, 3113. (e) Elangovan, A.; Lin, J.-H.; Yang, S.-W.; Hsu, H.-Y.; Ho, T.-I. *J. Org. Chem*. **2004**, *69*, 8086.

(5) (a) Makino, N.; Hoshi S.; Kitatani K. U.S. Patent 5093219, 1992. (b) Zhan, X.; Liu, Y.; Yu, G.; Wu, X.; Zhu, D.; Sun, R.; Wang, D.; Epstein, A. J. *J. Mater. Chem*. **2001**, *11*, 1606.

(6) (a) Suffert, J.; Ziessel, R. *Tetrahedron Lett*. **1991**, *32*, 757. (b) Chanteau, S. H.; Tour, J. M.; *Tetrahedron Lett*. **2001**, *42*, 3057. (c) Nakatsuji, S.; Matsuda, K.; Uesugi, Y.; Nakashima, K.; Akiyama S.; Fabian, W. *J. Chem. Soc., Perkin Trans. 1* **1992**, *7*, 755. (d) Schmidt-Mende, L.; Fechtenkötter, A.; Müllen, K.; Moons, E.; Friend, R. H.; MacKenzie, J. D. *Science*, **2001**, *293*, 1119. (e) Percec, V.; Glodde, M.; Bera, T. K.; Miura, Y.; Shiyanovskaya, I.; Singer, K. D.; Balagurusamy, V. S. K.; Heiney, P. A.; Schnell, I.; Rapp, A.; Spiess, H.-W.; Hudson S. D.; Duan, H. *Nature* **2002**, *419*, 384.

(7) (a) Holzapfel, M.; Lambert, C.; Selinka C.; Stalke, D. *Chem. Soc., Perkin Trans. 2* **2002**, *2*, 1553. (b) Nelsen, S. F. *Chem. Eur. J*. **2000**, *6*, 581. (c) Nelsen, S. F.; Adamus, J.; Wolff, J. J. *J. Am. Chem. Soc*. **1994**, *116*, 1589. (d) Launay, J.-P. *Chem. Soc. Rev*. **2001**, *30*, 386. (e) Lambert, C.; Nöll, G. *J. Am. Chem. Soc*. **1999**, *121*, 8434. (f) Lambert, C.; Nöll, G. *Angew. Chem., Int. Ed*. **1998**, *37*, 2107.

(8) (a) Onkelinx, A.; DeSchryver, F. C.; Viane, L.; Van der Auweraer, M.; Iwai, K.; Yamamoto, M.; Ichikawa, M.; Masuhara, H.; Maus M.; Rettig, W. *J. Am. Chem. Soc*. **1996**, *118*, 2892. (b) Onkelinx, A.; Shweitzer, F.; De Schryver, F. C.; Miyasaki, H.; Van der Auweraer, M.; Asahi, T.; Masuhara, H.; Fukumura, H.; Yashima A.; Iwai, K. *J. Phys. Chem. A* **1997**, *101*, 5054. (c) Maus, M.; Rettig, W.; Depaemelaere, S.; Onkelinx, A.; DeSchryver F. C.; Iwai. K. *Chem. Phys. Lett*. **1998**, *292*, 115. (d) Kapturkiewicz, A.; Herbich, J.; Karpiuk, J.; Nowacki, J. *J. Phys. Chem. A* **1997**, *101*, 2332. (e) Herbich J.; Kapturkiewicz, A. *J. Am. Chem. Soc*. **1998**, *120*, 1014 and references therein.

(9) (a) Faulkner, L. R.; Bard, A. J.. *Electrogenerated Chemiluminescence*; In *Electrochemical methods*; John Wiley & Sons: New York, 1980; pp 621−627. (b) Oyama, M.; Okazaki, S. *Anal. Chem*. **1998**, *70*, 5079. (c) Kapturkievicz, A. *J. Electroanal. Chem*. **1990**, *290*, 135. (d) Kapturkievicz, A. *J. Electroanal. Chem*. **1991**, *302*, 13. (e) Armstrong, N. R.; Whightman, R. M.; Gross, E. M. *Annu. Rev. Phys. Chem*. **2001**, *52*, 391. (f) Richter, M. M. *Chem. Rev*. **2004**, *104*, 3003. (g) Bard, A. J.; Faulkner, L. R. In *Electroanalytical Chemistry*; Bard, A. J., Ed.; Marcel-Dekker: New York, 1977; Vol. 10, p 3.

(10) (a) Anderson, J. D.; McDonald, E. M.; Lee, P. A.; Anderson, M. L.; Ritchie, E. L.; Hall, H. K.; Hopkins, T.; Mash, E. A.; Wang, J.; Padias, A.; Thayumanavan, S.; Barlow, S.; Marder, S. R.; Jabbour, G. E.; Shaheen, S.; Kippelen, B.; Peyghambarian, N.; Wightman, R. M.; Armstrong, N. R. *J. Am. Chem. Soc*. **1998**, *120*, 9646. (b) Armstrong, N. R.; Anderson, J. D.; Lee, P. A.; McDonald, E. M.; Wightman, R. M.; Hall, H. K.; Hopkins, T.; Padias, A.; Thayumanavan, S.; Barlow, S.; Marder, S. R. *SPIE* **1999**, *3476*, 178. (c) Ketter, J. B.; Wightman, R. M. *J. Am. Chem. Soc*. **2004**, *126*, 10183.

(11) Reynolds, G. A.; Drexhage, K. H. *Opt. Commun*. **1975**, *13*, 222.

(12) Fery-Forgues, S.; Lavabre, D. *J. Chem. Educ*. **1999**, *76*, 1260.

(13) (a) Elangovan, A.; Wang, Y.-H.; Ho, T.-I. *Org. Lett*. **2003**, *5*, 1841. (b) Sonogashira, K.; Tohda, Y.; Hagihara, N. *Tetrahedron Lett*. **1975**, *16*, 4467.

(14) (a) Lakovickz, J. R. *Principles of Fluorescence Spectroscopy;* Plenum Press: New York, 1983; p 187 (b) Lippert, Von E. *Z. Elektrochem*. **1957**, *61*, 962.

(15) Watson, A. T.; Matsen, F. A. *J. Chem. Phys*. **1950**, *18*, 1305.

(16) Faulkner, L. R.; Tachikawa, H.; Bard, A. J. *J. Am. Chem. Soc*. **1972**, *94*, 691.

(17) (a) Morsi, S. E.; Carr, D.; El-Bayoumi, M. A. *Chem. Phys. Lett*. **1978**, *58*, 571. (b) Ebeid, E. M.; El-Bayoumi, M. A.; Williams, J. O. *J. Chem. Soc., Faraday Trans 1* **1978**, *74*, 1457. (c) Kasha, M.; Rawls, H. R.; El-Bayoumi, M. A. *Pure Appl. Chem*. **1965**, *11*, 371.

(18) (a) Visco, R. E.; Chandross, E. A. *J. Am. Chem. Soc*. **1964**, *86*, 5350. (b) Chandross, E. A.; Longworth, J. W.; Visco, R. E. *J. Am. Chem. Soc*. **1965**, *87*, 3259. (c) Faulkner, L. R.; Bard, A. J. *J. Am. Chem. Soc*. **1968**, *90*, 6284. (d) Hercules, D. M. *Science* **1964**, *145*, 808.

(19) McVey, J. K.; Shold, D. M.; Yang, N. C. *J. Chem. Phys*. **1976**, *65*, 3375.

(20) Crystal data for **1**: Formula $C_{24}H_{19}N$; formula weight: 321.40; unit cell parameters with standard deviations (unit cell lengths in Å): cell length a, 9.2040(2) Å; cell length b, 9.3250(2) Å; cell length c, 11.0960(3) Å; cell angle α: 72.871(2)°; cell angle β: 80.4240 (10)°; cell angle γ: 71.4130(10)°; cell volume: 859.86 (4) Å^3; symmetry space group: H−M: P-1; cell formula units Z: 2; temperature of study: 295(2) K.; absorption coefficient: 0.072 mm^{-1}; reflections collected: 5163; independent reflections: 2982 (R_{int} = 0.0226); final R indices [$I > 2\sigma(I)$]: R1 = 0.0451, wR2 = 0.1232; R indices (all data): R1 = 0.0582, wR2 = 0.1361.

(21) (a) Birks, J. B. *Photophysics of Aromatic Molecules*; Wiley-Interscience: New York, 1970. (b) Beens, H.; Weller, A. In *Organic Molecular Photophysics*; Birks, J. B., Ed.; John-Wiley & Sons: London, 1975; p 198.

(22) All calculations were performed using *Spartan '04* for Windows, Wavefunction Inc., 18401 Von Karman Avenue, Suite 370, Irvine, CA 92612. (a) Hehre, W. J. *A guide to Molecular Mechanics and Quantum Chemical Calculations*; Wavefunction Inc.: Irvine, CA, 2003. (b) Lee, C.; Yang, W.; Parr, R. G. *Phys. Rev. B* **1988**, *37*, 785. (c) Beck, A. D. *J. Chem. Phys*. **1993**, *98*, 5648.

(23) (a) *Handbook of Organic Solvents*; Lide, D. R., Ed.; CRC Press: Boca Raton, FL, 1995. (b) Dean, J. A. *Lange's handbook of chemistry*, 14th ed.; McGraw-Hill: New York, 1992; pp 1.190, 5.104.